JOURNAL OF SPACECRAFT AND ROCKETS
Vol. 46, No. 5, September–October 2009

Predicting the Perforation Response of Honeycomb Sandwich Panels Using Ballistic Limit Equations

William P. Schonberg*
Missouri University of Science and Technology, Rolla, Missouri 65409
and
Frank Schäfer† and Robin Putzar‡
Fraunhofer Institute for High-Speed Dynamics, 79104 Freiburg, Germany

DOI: 10.2514/1.41772

Man-made debris from previous spacecraft missions poses a serious threat to spacecraft that are launched to operate in Earth orbit because it can strike such spacecraft at extremely high velocities and consequently damage mission-critical systems. Most satellites are constructed with honeycomb sandwich panels as their primary structural elements. To be able to perform a risk analysis, it is important to know, in the event of such a meteoroid or orbital debris particle impact, whether or not the impacting particle or parts thereof will exit the rear of the sandwich panel. A recently developed set of ballistic limit equations for two different types of honeycomb sandwich panels are studied to determine how well they perform when they are applied to systems that are outside of the database that was used to develop them. It was found that these ballistic limit equations are fairly conservative; they successfully predicted sandwich panel perforation in nearly all of the tests that resulted in perforation, while allowing approximately half of the nonperforating tests to be incorrectly labeled as tests with a perforation. This indicates the likelihood that use of these equations in design applications could result in overly robust shielding hardware.

Nomenclature

d_c	=	critical projectile diameter for failure of rear wall, cm
d_p	=	projectile diameter, cm
K_{MLI}	=	adjustment factor for multilayer insulation
K_{S2}	=	adjustment factor for scaling standoff distance S_2 in the hypervelocity regime
K_{tw}	=	adjustment factor for equipment cover plate thickness t_w in the hypervelocity regime
$K_{3\mathrm{D}}$, $K_{3\mathrm{S}}$	=	ESA triple-wall ballistic limit equation fit factors for the hyperballistic and ballistic velocity regimes, respectively
S_1, S_2	=	standoff between first and second, and second and third bumper, where third bumper = backwall, cm
t_b	=	thickness of the inner/second bumper (the rear face sheet in the case of a honeycomb sandwich panel), cm
t_{ob}	=	thickness of the outer bumper (the front face sheet in the case of a honeycomb sandwich panel), cm
t_w	=	thickness of third bumper/back wall/equipment cover plate, cm
V, V_n	=	impact velocity and its normal component ($V \cdot \cos\theta$), respectively, km/s
V_{t1}	=	transition velocity between ballistic and shatter velocity regimes, km/s
V_{t2}	=	transition velocity between shatter and hypervelocity regimes, km/s
$V_{t1,n}$, $V_{t2,n}$	=	normal component of $V_{t1} \cdot \cos\theta$ and $V_{t2} \cdot \cos\theta$, respectively, km/s
α, β, γ, δ, ε	=	fit parameters for the Schäfer–Ryan–Lambert ballistic limit equation
θ	=	impact angle (0 deg is a perpendicular impact on the target surface), deg
ρ_{ob}, ρ_p	=	volumetric density of the outer bumper and the projectile, respectively, g/cm^3
$\sigma_{y,\mathrm{ksi}}$	=	yield stress of the equipment cover plate, ksi

I. Introduction

THE near-Earth space environment is cluttered with man-made debris from previous spacecraft missions into that environment as well as with naturally occurring meteoroids. This debris poses a serious threat to spacecraft that are launched to operate in Earth orbit because it can strike such spacecraft at very high velocities and consequently damage mission-critical systems. As a result, as a spacecraft design evolves, the spacecraft designers must be aware of the response of various spacecraft components and structural elements under high-speed impact loading conditions. Precautions must be taken to ensure that a spacecraft's operation and functional units are not compromised when it is struck by an orbital debris particle or by a meteoroid.

Most satellites launched into Earth orbit are constructed with honeycomb sandwich panels (HC/SPs) as their primary structural load bearing elements. A typical honeycomb sandwich panel is shown in Fig. 1. Behind such panels are located spacecraft components that are appropriate for the particular spacecraft or satellite mission and function (e.g., electronics, avionics, fuel cells, pressure vessels, etc.).

To be able to perform a risk analysis for a particular satellite under a specific mission profile, it is important to know more than just whether or not the satellite will be struck by a meteoroid or an orbital debris particle. It is equally important to know, in the event of such an impact, whether or not the impacting particle (or its remnants) will exit the rear of the HC/SP (i.e., whether or not the ballistic limit of the HC/SP will be exceeded).

Although the response of a multiwall system with monolithic flat panel walls under high-speed particle impact has been studied extensively over the past 50 years or so, the extent of the effort to study HC/SPs under similar impact conditions has been much more limited. The issue of whether or not the ballistic limit of a HC/SP will be exceeded under a given set of impact conditions has been

Received 23 October 2008; revision received 30 April 2009; accepted for publication 26 June 2009.

*Professor and Department Chair, Civil, Architectural, and Environmental Engineering Department, 1401 North Pine Street. Associate Fellow AIAA.
†Head, Spacecraft Technology Group, Ernst Mach Institute, Eckerstraße 4.
‡Senior Scientist, Spacecraft Technology Group, Ernst Mach Institute, Eckerstraße 4.

Fig. 1 Generic honeycomb sandwich panel with aluminum face sheets.

examined recently by several investigators. As a result of these efforts, a set of ballistic limit equations (BLEs) have been developed for different types of HC/SPs to model whether or not perforation of the rear wall of an HC/SP will occur. These BLEs define the threshold particle size that will cause perforation of the HC/SP rear wall as a function of variables known to affect the ballistic limit, namely, impact velocity and angle, particle density and shape, HC/SP thickness, and the thicknesses and material properties of the front face sheet, HC/SP core, and rear face sheet.

Ballistic limit equations are typically drawn as ballistic limit curves (BLCs) that define lines of demarcation between regions of rear wall perforation and no perforation for a given HC/SP under consideration and are primarily based on rear face sheet perforation/nonperforation data obtained from hypervelocity impact tests. In particular, impact testing using spherical projectiles fired in light gas guns typically provides the data for these HC/SP BLCs at impact velocities between 3 and 7 km/s. These data are then fitted with scaled single-wall equations below 3 km/s and with theoretical momentum/energy based penetration relationships above 7 km/s to obtain standard three-part BLCs that cover the full range of impact velocity, that is, from approximately 0.5 to 16 km/s.

There are some drawbacks to using empirically derived BLEs for spacecraft shielding design, especially those derived using the heuristic process already described. One major drawback is that BLEs derived in this fashion are not statistically based; they are not curve fits, but rather are simply lines of demarcation between regions of penetration and nonpenetration. As a result, it is not possible to obtain uncertainty bounds and/or confidence intervals as part of the current procedure that is used to derive them. Another drawback is that these BLEs are derived in terms of a critical projectile diameter, because the testing performed to supply the data for their development is almost exclusively performed using spherical projectiles. However, orbital debris particles and meteoroids are not spherical and, as such, might be better modeled by other regular or irregular solids [1]. However, it is the current practice to use these equations, derived in the manner already described, for the purpose of shielding design by nearly all space-faring communities. Dialogues and studies are ongoing to address some of these drawbacks and limitations (see, for example, [1]), but until these issues are resolved, there is simply no other alternative approach as efficient as the one currently being used.

It is equally important to note that the empirical nature of these HC/SP BLEs subjects them to potential inaccuracy, particularly when applied to HC/SP configurations that have not been well tested. Of course, extrapolating empirical equations to conditions beyond those and for configurations other than those for which the data on which they are based has been obtained can be a dangerous practice. However, the fact remains that every single possible wall configuration that can be conceived cannot be tested thoroughly for the purposes of developing a multitude of configuration-specific BLEs. Empirical equations *are* used beyond the parameters of their underlying databases, and they *are* used for (related) configurations not tested in their development. Our curiosity was piqued, and the following question naturally arose: just how well do these new BLEs perform when they are applied to HC/SP systems that are outside of the parameters of the test database that was used to develop them? The results provided in this paper answer this question.

The ballistic limit equations of interest in this study are those for aluminum and composite HC/SPs that have been recently developed and can be found in [2,3], respectively. These equations are typically referred to as the Schäfer–Ryan–Lambert (SRL) BLEs for HC/SPs. In [2] the SRL BLEs for aluminum HC/SPs are given by Eqs. 1–3, whereas in [3] those for composite HC/SPs are given by Eqs. 4–6. Actually, these equations have been developed for predicting the penetration threshold of spacecraft equipment inside the spacecraft, assuming the impact of particles that are energetic enough to perforate a HC/SP spacecraft structural wall and generate fragments that are energetic enough to impinge on the equipment outer wall and to cause damage to it. Although these equations can be applied to calculate the BL of the compound system of the satellite structure wall plus equipment front wall, they also allow the calculation of the BL of a stand-alone sandwich panel spacecraft structure, a feature that has been used for the analysis reported in this paper. To assess how well these equations perform in terms of predicting perforation (P) or nonperforation (NP) of the respective HC/SP systems, an exercise was undertaken to compare the P/NP predictions of the equations in [2,3] against actual P/NP occurrences as found in the data from a variety of previous experimental investigations.

II. Overview of Honeycomb Sandwich Panel Schäfer–Ryan–Lambert Ballistic Limit Equations

For completeness, the SRL ballistic limit equations are presented before reducing them to the equations that have been used for the analysis in this paper. As outlined in Sec. I, these ballistic limit equations needed to be capable of considering explicitly the thicknesses, materials, and spacing of three plates (Fig. 2). The first and the second plates represent the spacecraft's structure wall (e.g., the honeycomb sandwich panel of a satellite or the bumper and primary structure of a manned spacecraft), whereas the third plate represents the back wall of a multiwall system or the front wall or cover plate of the equipment under consideration (see [2]).

As a failure criterion for the equation, the criterion proposed by Christiansen [4] for the rear wall of a Whipple shield was adopted: failure is defined as either a through hole in the sandwich panel's rear face sheet or in the equipment cover plate or as a detached spall from either the sandwich panel's rear face sheet or the equipment cover plate's rear side, respectively, depending on the test configuration (*even in the absence of a through hole*). This is a conservative definition of failure and used mostly likely because the BLEs developed by Christiansen were planned for use on the International Space Station, where human lives are at stake. It is with this definition in mind that this study was performed; the results of this study and its main conclusions could change, of course, if this definition of failure were relaxed somewhat, so as, for example, to include only a through-hole perforation.

A. Schäfer–Ryan–Lambert Ballistic Limit Equations

The SRL BLEs uses a notation similar to the one introduced by ESA [5], in which several coefficients are adjusted to fit to the experimental ballistic limit data. The following equation yields the

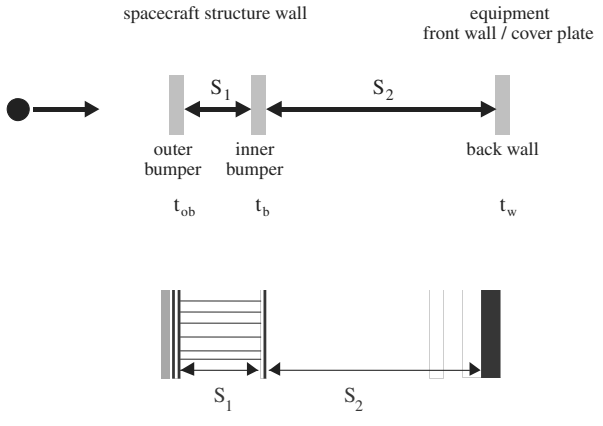

Fig. 2 Principle setup for SRL ballistic limit equation geometry.

critical projectile diameter as a function of impact velocity in the ballistic velocity regime ($V_n \le V_{t1,n}$):

$$d_c(V) = \left[\frac{\frac{(t_w^{\alpha}+t_b)}{K_{3S}}\left(\frac{\sigma_{y,\mathrm{ksi}}}{40}\right)^{1/2} + t_{\mathrm{ob}} + K_{\mathrm{MLI}}\cdot t_{\mathrm{eq,MLI}}}{0.6\cdot(\cos\theta)^{\delta}\cdot\rho_p^{1/2}\cdot V^{2/3}}\right]^{18/19} \qquad (V_n \le V_{t1,n}) \tag{1}$$

where MLI refers to multilayer insulation.

In this regime, it is assumed that the projectile does not fragment; hence, the protection offered by the target essentially stems from the amount of mass in the line of sight of the projectile. To allow experimental data to be fitted to the equation, the power of α has been added to the wall thickness of the equipment cover plate t_w. Furthermore, a term to take care of the protection enhancement from the MLI ($K_{\mathrm{MLI}}\cdot t_{\mathrm{eq,MLI}}$) has been added, where $t_{\mathrm{eq,MLI}}$ is the equivalent thickness of the MLI.

In the shatter velocity regime ($V_{t1,n} < V_n < V_{t2,n}$), a linear extrapolation is made for the critical projectile diameter, d_c, between the ballistic regime, Eq. (1), and the hypervelocity regime, Eq. (3), according to the following equation:

$$d_c(V) = d_c(V_{t1}) + \frac{d_c(V_{t2}) - d_c(V_{t1})}{V_{t2} - V_{t1}}\cdot(V - V_{t1}) \quad (V_{t1,n} < V_n < V_{t2,n}) \tag{2}$$

The following equation describes the critical projectile diameter for the failure of the rear wall, d_c, in the hypervelocity regime ($V_n \ge V_{t2,n}$):

$$d_c(V) = \frac{1.155\cdot S_1^{1/3}\cdot(t_b + K_{tw}\cdot t_w)^{2/3} + K_{S2}\cdot S_2^{\beta}\cdot t_w^{\gamma}\cdot(\cos\theta)^{-\varepsilon}\cdot\left(\frac{\sigma_{y,\mathrm{ksi}}}{70}\right)^{1/3}}{K_{3D}^{2/3}\cdot\rho_p^{1/3}\cdot\rho_{\mathrm{ob}}^{1/9}\cdot V^{2/3}\cdot\cos\theta^{\delta}} \quad (V_n \ge V_{t2,n}) \tag{3}$$

In the equation for the critical projectile diameter in the hypervelocity regime ($V_n \ge V_{t2,n}$), Eq. (3), the term $K_{S2}\cdot S_2^{\beta}\cdot t_w^{\gamma}\cdot(\cos\theta)^{-\varepsilon}$ has been added to explicitly consider equipment placed behind an HC/SP structural wall. The cosine factor introduced in this part of the equation was necessary to reflect an experimentally observed considerable increase in critical projectile diameters in the hypervelocity regime at oblique impacts. The data obtained also suggest that the standoff S_2 contributes significantly to the enhancement of the protection capability at hypervelocity. Fit factor K_{S2} is required to balance the term $S_2^{\beta}\cdot t_w^{\gamma}\cdot(\cos\theta)^{-\varepsilon}$, as all fit parameters, K_{S2}, β, γ, and ε, are interrelated. Hence, changing one fit parameter requires adjustment of at least one of the other parameters.

In addition, a term consisting of the thickness, t_w, of the equipment cover plate multiplied by a fit factor, K_{tw}, has been added to t_b. The expanded term $t_b + K_{tw}\cdot t_w$ represents an effective thickness of the inner bumper and the equipment cover plate. Its significance becomes apparent when considering a case in which the equipment is mounted directly on the inner bumper of the structure wall (i.e., when $S_2 = 0$). This case essentially corresponds to a Whipple shield with a single bumper and a rear wall consisting of the inner bumper and the equipment cover plate. It can be shown that the penetration resistance of two plates with zero spacing is larger than the penetration resistance of a plate with a thickness equal to the sum of the thicknesses of the two plates. This can be explained by shock wave reflection at the interface of the two plates, which effectively increases the penetration resistance of the wall to impacting fragments. With K_{tw} as a fit factor to impact experiments, this effect can be considered.

To apply Eqs. (1–3) to the calculation of a BLC of a stand-alone honeycomb sandwich panel structure wall, t_w and S_2 are set to 0. In this case, the space-facing (front) face sheet of the sandwich panel corresponds to the outer bumper (t_{ob}), whereas the rear face sheet corresponds to the inner bumper, t_b; its thickness is the standoff distance S_1. The effect of the honeycomb core on the protection capability is taken into account by the fit coefficients and the $\cos\theta$ angle dependence of the BLE. It is interesting to note that under these conditions (i.e., $t_w = 0$ and $S_2 = 0$), the form of the SRL BLEs reduces to that of the Whipple shield equation [4] as well as that of the ESA triple-wall equation [5], respectively. Term-by-term equivalence can be obtained with $K_{3S} = 1$ and $K_{\mathrm{MLI}} = 0$ in the shatter velocity regime and $K_{3D} = 0.16$ in the hypervelocity velocity regime, as shown in [2,3].

Table 1 Fit parameters for SRL BLEs with aluminum and CFRP face sheets

Fit parameter	Aluminum HC/SP	CFRP HC/SP
K_{3S}	1.40	1.1
K_{3D}	0.4	0.4
K_{MLI}	3.0	0
K_{S2}	0.1	1.0
K_{tw}	1.5	1.0
α	1/2	1/2
β	2/3	1/3
γ	1/3	2/3
δ	4/3, $\theta \le 45$ deg, $\theta \ge 65$ deg	
	5/4, 45 deg $< \theta <$ 65 deg	4/3
ε	8/3, $\theta \le 45$ deg, $\theta \ge 65$ deg	
	10/4, 45 deg $< \theta <$ 65 deg	0
$v_{t1,n}$	3 km/s	4.2 km/s
$v_{t2,n}$	7 km/s	8.4 km/s

Because the SRL equation has been fit mostly to test data obtained in normal impact tests (i.e., at $\theta = 0$ deg), it is most valid for normal impacts. In the event that MLI is placed on the outward-facing face sheet of the honeycomb sandwich panel, the face sheet thickness t_{ob} is increased by an amount of aluminum equal to the mass of the MLI, $t_{\mathrm{eq,MLI}}$, multiplied by an adjustment factor, K_{MLI}, which always exceeds 1. This adjustment factor takes into account the effective improvement of protection typically observed whenever

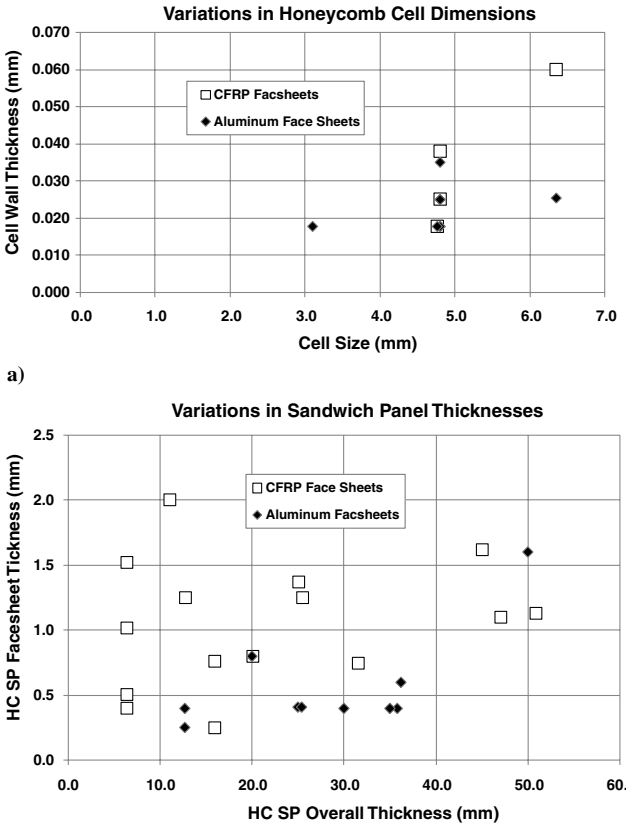

Fig. 3 Shown are the following: a) variations in HC/SP honeycomb cell dimensions, b) variations in HC/SP overall and face sheet thicknesses.

MLI is placed on the outside of the outermost structure wall. In this case, the MLI behaves as a thin multishock shield. The quantity $t_{\text{eq,MLI}}$ is given by the ratio $\rho_{\text{AD,MLI}}/\rho_{\text{ob}}$, where $\rho_{\text{AD,MLI}}$ is the areal density of the MLI (in grams per square centimeter).

B. Fit Coefficients for Use with Aluminum and Carbon Fiber Reinforced Polymer Honeycomb Sandwich Panels

The various fit parameters for Eqs. (1–3) as obtained from the curve-fitting exercise for each type of HC/SP are given in Table 1. We note that, in a carbon fiber reinforced polymer (CFRP) HC/SP, the rear face sheet thickness t_b is calculated according to the equation $t_b = t_{b,\text{CFRP}} \cdot (\rho_{\text{CFRP}}/2.78)$, where $t_{b,\text{CFRP}}$ is the thickness of the CFRP face sheet, and ρ_{CFRP} is the volumetric density of the CFRP; the value of 2.78 corresponds to the reference density of aluminum. The thickness of the front face sheet in a CFRP HC/SP is calculated in a similar manner, namely, $t_{\text{ob}} = t_{\text{ob,CFRP}} \cdot (\rho_{\text{CFRP}}/2.78)$. In addition, in Eq. (3), for a CFRP HC/SP, σ_y is actually $\sigma_{y,\text{AL}}$ and ρ_{ob} is actually ρ_{AL}.

III. Assessment of Honeycomb Sandwich Panel Schäfer–Ryan–Lambert Ballistic Limit Equations

Results from over 320 hypervelocity impact tests from 15 different test programs conducted in the United States and Europe were used to assess how well the SRL BLEs were able to predict P/NP events for a wide variety of HC/SP systems. In this manner, that is, by not using data from just one source and by not referring to only a few configurations of the same materials, we have reduced the possibility of introducing systematic errors or biases in the application of the SRL BLEs. Figures 3a and 3b show a distribution of the HC/SP geometric parameters considered in this study. This range of parameters is typical of those used in current satellite construction.

Figures 4 and 5 demonstrate the ability of the SRL BLEs to predict failure or nonfailure for HC/SPs with aluminum and composite face

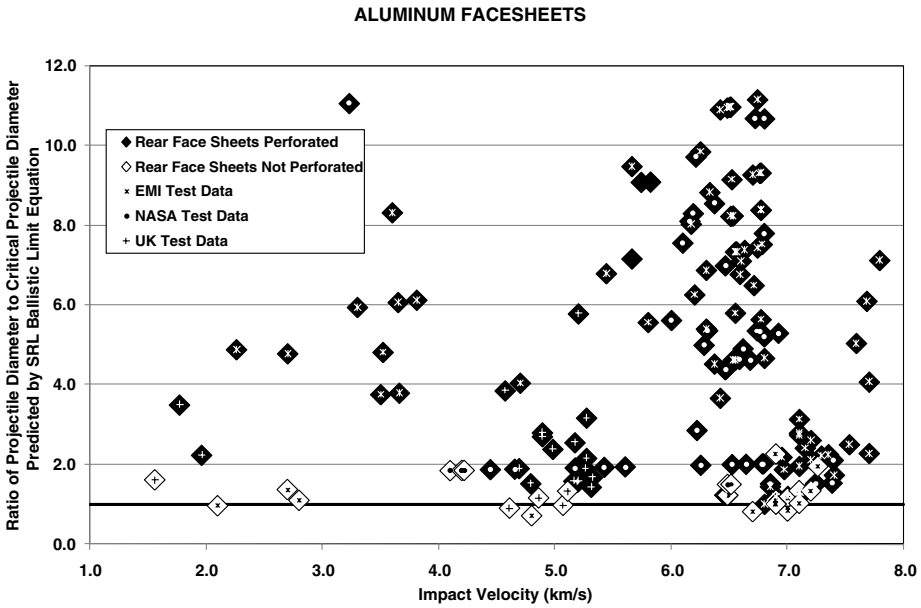

Fig. 4 Prediction of HC SP perforation and nonperforation using the SRL BLEs for aluminum face sheets.

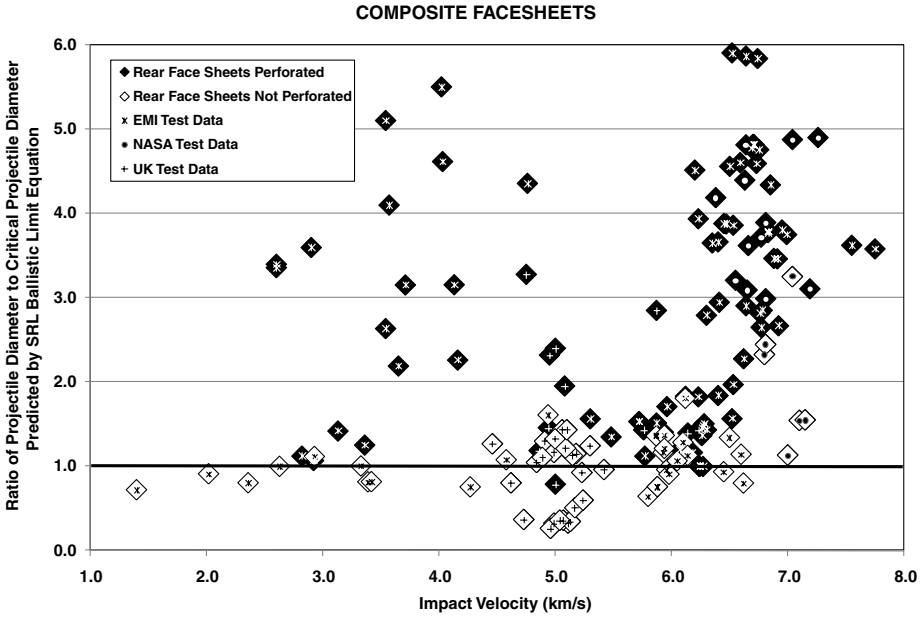

Fig. 5 Prediction of HC/SP perforation and nonperforation using the SRL BLEs for composite face sheets.

Table 2 Ability of SRL BLEs to predict HC/SP rear face sheet fails or passes

Tests without rear face sheet failure/perforation			Tests with rear face sheet failure/perforation		
Al face sheets	No. passes predicted	7	Al face sheets	No. fails predicted	135
	No. passed	29		No. failed	135
	Success rate, %	24.1		Success rate, %	100
CFRP face sheets	No. passes predicted	24	CFRP face sheets	No. fails predicted	101
	No. passed	59		No. failed	104
	Success rate	40.7%		Success rate	97.1%
Total	No. passes predicted	31	*Total*	No. fails predicted	236
	No. passed	88		No. failed	239
	Success rate, %	35.2		Success rate, %	98.7

Table 3 Signal theory representation of SRL BLE performance

Al face sheets		
TP = 135 (100%)	FP = 22	157
FN = 0	TN = 7 (24.1%)	7
135	29	164
CFRP face sheets		
TP = 101 (97.1%)	FP = 35	136
FN = 3	TN = 24 (40.7%)	27
104	59	163
Total		
TP = 236 (98.7%)	FP = 57	293
FN = 3	TN = 31 (35.2%)	34
239	88	327

sheets, respectively, as a function of velocity based on the data noted in Sec. II. Solid markers indicate inner wall failure, whereas hollow markers indicate nonfailure. The velocity axis shows the component of the projectile velocity that is normal to the shield surface. The information for HC/SPs with aluminum face sheets is obtained from [2,6–10], whereas that for HC/SPs with composite face sheets comes from [3,11–16]. In these figures, the sources of the data have been identified in general terms with regard to the organization performing the tests noted in those figures.

In Figs. 4 and 5, solid markers *above* the dark horizontal line correspond to tests having HC/SP failures/perforations caused by projectiles with diameters larger than the predicted ballistic limit diameters and indicate successful predictions by the corresponding SRL BLEs (true positives, or hits, to borrow some terminology from signal processing theory, assuming that a rear face sheet failure/perforation is considered to be a "positive" test result). Conversely, a solid marker *below* the dark horizontal line corresponds to a test with HC/SP failure/perforation caused by a projectile with a diameter smaller than the predicted ballistic limit diameter and indicates a nonsuccessful prediction (that is, the BLE predicted nonperforation of the HC/SP, but instead perforation did occur). These would be considered false negatives or misses.

Similarly, hollow markers *above* the dark horizontal line correspond to tests without HC/SP failures/perforations but with projectiles with diameters larger than the predicted ballistic limit diameters and indicate nonsuccessful predictions by the BLE (that is, the BLE predicted HC/SP perforation, but it did not occur). These would be considered as false positives or false alarms. Conversely, hollow markers *below* the dark line correspond to tests without HC/SP failures/perforations and with projectiles with diameters smaller than the predicted ballistic limit diameters and indicate successful predictions (that is, true negatives or correct rejections).

As can be seen from Figs. 4 and 5, the SRL BLEs for HC/SPs with both aluminum and composite face sheets are indeed fairly conservative: they successfully predict HC/SP perforation in nearly all of the tests that did result in perforation, while allowing nearly two-thirds of the nonperforating tests to be incorrectly labeled as tests with a perforation of the HC/SP. Table 2 summarizes the failure and nonfailure prediction success rates of the SRL BLEs for the tests and HC/SP configurations considered in this study. The information in Table 2 reinforces the visual observations regarding the ability of the SRL BLEs to predict perforation or nonperforation of the rear face sheet of an HC/SP. In Table 2, a "pass" is a test without rear face sheet failure/perforation, whereas a "fail" is a test that has sustained rear face sheet failure/perforation.

The information in Table 2 is presented in a more compact form in Table 3 using the conventions borrowed from signal theory (e.g., TP = true positive, TN = true negative, FP = false positive, and FN = false negative).

IV. Conclusions

Considering the wide variety of test data sources and the differing objectives of the test programs that produced that data, it was a bit surprising to see the SRL BLEs so consistently conservative in their predictions. As such, if they are used in spacecraft design applications they could result in overly robust shielding hardware. The conservative nature of these equations could result in a mass penalty for spacecraft that would be able to withstand failure from impacts that are just as likely to not result in failure. However, if the design is relaxed, then the penalty might be in the form of an increased likelihood of spacecraft loss due to failure from impacts that were considered to not result in failure. Mitigation of this overly robust potential while still assuring adequate design requires additional hypervelocity testing to "tune" these BLEs for the specific hardware under consideration. The results obtained in this study are especially relevant for space programs, especially those involving habitable spacecraft, that cannot afford to either overpredict (because of weight considerations) or underpredict (because of risk considerations) the damage from anticipated meteoroid or orbital debris impacts.

The question of what can or should be done to render the SRL BLEs more "accurate" naturally arises as well; however, the use of the word accurate implies the existence of some absolute metric against which the performance of a BLE can be measured. Unfortunately, no such metric exists. However, what *can* be done is to modify the SRL BLEs, for example, to make it "less conservative." A straightforward way to effect such a change would be to simply increase the predicted critical projectile diameter across the board by, for example, 10%. The result of this would be to "lower" all the points in Figs. 4 and 5; more perforations would be predicted as nonperforations (more solid markers would be below the horizontal line at 1.0), and fewer nonperforations would be predicted as perforations (more hollow markers would be below the horizontal line at 1.0). This might convey the impression of the revised version of the BLE as being "more accurate," but, in reality, it be would only appropriate to call it less conservative.

Acknowledgments

W.P. Schonberg is grateful for the support provided by the Humboldt Foundation through a Fraunhofer–Bessel Research Award that enabled this study. The Schäfer–Ryan–Lambert ballistic limit equations have been developed under European Space Research and Technology Centre contracts 16721/02 and 16483/02.

References

[1] Squire, M., "Independent Review of Constellation (Cx) Orion Vehicle Micrometeroids and Orbital Debris (MMOD) Risk Analysis," NASA Engineering and Safety Center Rept. NESC-RP-08-00468, Jan. 2009.

[2] Schäfer, F. K., Ryan, S., Lambert, M., and Putzar, R., "Ballistic Limit Equation for Equipment Placed Behind Satellite Structure Walls," *International Journal of Impact Engineering*, Vol. 35, No. 12, 2008, pp. 1784–1791. doi:10.1016/j.ijimpeng.2008.07.074

[3] Ryan, S., Schäfer, F., Destefanis, R., and Lambert, M., "A Ballistic Limit Equation for Hypervelocity Impacts on Composite Honeycomb Sandwich Panel Satellite Structures," *Advances in Space Research*, Vol. 41, No. 7, 2008, pp. 1152–1166. doi:10.1016/j.asr.2007.02.032

[4] Christiansen, E. L., "Design and Performance Equations for Advanced Meteoroid and Debris Shields," *International Journal of Impact Engineering*, Vol. 14, 1993, pp. 145–156. doi:10.1016/0734-743X(93)90016-Z

[5] Drolshagen, G., and Borge, J., "ESABASE/DEBRIS: Meteoroid/ Debris Impact Analysis Technical Description, Issue 1 for ESABASE version 90.1," European Space Research and Technology Centre Rept. ESABASE-GD-01/1, Noordwijk, The Netherlands, 1992.

[6] "Effectiveness of Aluminum Honeycomb Shields in Preventing Meteoroid Damage to Liquid-Filled Spacecraft Tanks," NASA CR-65261, 1964.

[7] Shephard, G. L., and Scheer, S. A., "Secondary Debris Impact Damage and Environment Study," *International Journal of Impact Engineering*, Vol. 14, 1993, pp. 671–682. doi:10.1016/0734-743X(93)90062-C

[8] Frate, D. T., and Nahra, H. K., "Hypervelocity Impact Testing of Nickel-Hydrogen Battery Cells," AIAA Paper 96-4292, 1996; also NASA TM-107325.

[9] Turner, R. J., Taylor, E. A., McDonnell, J. A. M., Stokes, H., Marriott, P., Wilkinson, J., Catling, D. J., Vignjevic, R., Berthold, L., and Lambert, M., "Cost Effective Debris Shields for Unmanned Spacecraft," *International Journal of Impact Engineering*, Vol. 26, 2001, pp. 785–796. doi:10.1016/S0734-743X(01)00131-2

[10] Lambert, M., Schäfer, F., and Geyer, T., "Impact Damage on Sandwich Panels and Multi-Layer Insulation," *International Journal of Impact Engineering*, Vol. 26, 2001, pp. 369–380. doi:10.1016/S0734-743X(01)00108-7

[11] Frost, C. L., and Rodriguez, P. I., "AXAF Hypervelocity Impact Test Results," *Proceedings of the 2nd European Conference on Space Debris*, SP-393, ESA, Paris, 1997, pp. 423–428.

[12] Taylor, E. A., Herbert, M. K., Gardner, D. J., Kay, L., Thomson, R., and Burchell, M. J., "Hypervelocity Impact on Spacecraft Carbon Fiber Reinforced Plastic/Aluminum Honeycomb," *Proceedings of The Institution of Mechanical Engineers Part G Journal of Aerospace Engineering*, Vol. 211, No. 5, 1997, pp. 355–363. doi:10.1243/0954410971532721

[13] Taylor, E. A., "Cost Effective Debris Shields for Unmanned Spacecraft," *Proceedings of the Hypervelocity Impact Shielding Workshop*, Inst. for Advanced Technologies, Austin, Texas, 1998, pp. 139–150.

[14] Schäfer, F., Destefanis, R., Ryan, S., Riedel, W., and Lambert, M., "Hypervelocity Impact Testing of CFRP/AL Honeycomb Satellite Structures," *Proceedings of the 4th European Conference on Space Debris*, SP-587, ESA, Paris, 2005, pp. 407–412.

[15] Schäfer, F., "Composite Materials Impact Damage Analysis," Fraunhofer Ernst Mach Institute, Rept. I-83-05, Freiburg, Germany, 2005.

[16] Ryan, S., Schäfer, F., and Riedel, W., "Numerical Simulation of Hypervelocity Impact on CFRP/Al HC SP Spacecraft Structures Causing Penetration and Fragment Ejection," *International Journal of Impact Engineering*, Vol. 33, 2006, pp. 703–712. doi:10.1016/j.ijimpeng.2006.09.072

L. Peterson
Associate Editor